Frontiers of Physics
https://doi.org/10.1007/s11467-019-0931-2
Front. Phys.
15(2), 21601 (2020)

RESEARCH ARTICLE

Error-detected N-photon cluster state generation based on the controlled-phase gate using a quantum dot in an optical microcavity

Lei-Xia Liang[1,*], Yan-Yan Zheng[1,2,*], Yuan-Xia Zhang[1], Mei Zhang[1,†]

[1] *Department of Physics, Applied Optics Beijing Area Major Laboratory, Beijing Normal University, Beijing 100875, China*
[2] *School of Physics and Electronic Information, Yan'an University, Yan'an 716000, China*
Corresponding author. E-mail: [†] *zhangmei@bnu.edu.cn*

Received August 4, 2019; accepted September 10, 2019

We propose a scheme for error-detected generation of an N-photon cluster state with a quantum dot (QD) embedded in a single-sided optical microcavity (QD-cavity system). The basic structure of this scheme is an error-detected controlled-phase (C-phase) gate on the hybrid electron–photon system. In this scheme, the fidelity of N-photon cluster state generation can be reached unity even if low-Q cavity and cavity leakage are considered. By using error detecting, the generation of an N-photon cluster state can be performed by repeating until success, which also leads to a high success probability, compared with other schemes assisted by the QD-cavity system. The error-detected generation of an N-photon cluster state in the highly controllable way may benefit on the quantum network in the future.

Keywords controlled-phase gate, cluster state, error-detected, QD-cavity system

1 Introduction

Quantum computing has attracted widespread attention because of its great superiority in speed and operation. Quantum computers can handle some tasks that are difficult for classic computers [1–6]. Quantum Entanglement plays an important role in quantum computation and quantum gates, including the gates based on nuclear magnetic resonance [7], holonomic quantum computation [8–11], quantum dots [12–15], diamond nitrogen vacancy centers [16, 17], superconducting qubits [18–20], photons based on polarization states [21–26], hyperparallel photonic quantum gates [27–33], atom systems [34–36], and one-way quantum computation [37]. It is also an important resource in quantum communication, such as quantum key distribution [38–40], quantum secret sharing [41], quantum secure direct communication [42–47], quantum teleportation [48], quantum dense coding [49, 50], and quantum repeater [51–56] in which there are five core techniques for its application, including entanglement generation [57–59], entanglement distribution [60–64], entanglement purification [65–76] and entanglement concentration [77–85], entanglement swapping with entangled-state analysis [86–95], and quantum state storage.

The quantum cluster state, a special type of N-qubit entangled state, was introduced by Briegel and Raussendorf [96] in 2001. The cluster state owns the advantages of Greenberger–Horne–Zeilinger (GHZ) and W-class entangled states and has been used for one-way quantum computation [97–100]. A series of theoretical and experimental schemes for generating the cluster state have been proposed [59, 101–105]. In 2005, Borhani and Loss [101] proposed a scheme for creating a cluster state with Heisenberg interactions. In 2008, Tokunaga *et al.* [102] experimentally demonstrated a four-photon cluster state by using two single photons and an entangled photon pair with a high fidelity. In the same year, Yukama *et al.* [103] achieved four-mode continuous-variable cluster states experimentally. In 2009, Ceccarelli *et al.* [59] created a six-qubit linear cluster state with a two-photon hyperentangled state. In this hyperentangled cluster state, three qubits are encoded in each particle, one in the polarization and two in the linear momentum degrees of freedom. In 2011, Yu *et al.* [104] proposed schemes for generating photon and electron-spin cluster states based on C-phase gate by using QD-cavity system. In 2016, Zhang *et al.* [105] demonstrated a high-fidelity four-photon cluster state in experiment via a spontaneous parametric down-conversion process. The scheme can be directly extended to more photons to generate an N-qubit linear cluster state. To generate a $2N$-qubit linear cluster state from N pairs of entangled photons, only $(N-1)$ Hong–Ou–Mandel interferences are needed. The success probability for 2N-qubit cluster state can reach $(\frac{1}{4})^N$. Recently, cluster states can be created by many different physical systems, such as nitrogen–vacancy (NV) center, superconducted circuits, quantum dots, and so on.

Recently, an electron spin in a single charged quan-

∗The first two authors contributed equally to this work.

© Higher Education Press and Springer-Verlag GmbH Germany, part of Springer Nature 2020

tum dot (QD) has been increasingly widespread in quantum computation [106–109], quantum network [110], and quantum information processing [111]. QD-cavity system generally includes to two different types: one is a quantum dot embedded in a single-sided optical microcavity, and the other involves a double-sided optical microcavity. With its long electron-spin coherence time [112–116], fast manipulation, and easy initialization [117–119], in recent years, QD-cavity system has developed greatly in both theoretical and experimental field [104, 120–122]. In 2008, Hu *et al.* proposed two schemes to entangle two remote spins [120] and realise photon entangler [121]. In 2011, Yu *et al.* [104] proposed schemes for constructing a controlled-phase gate and cluster states with single charged QDs in the strong-coupling regime. In ideal condition, the fidelity of the generation of cluster states can reach unity one. However, in practical condition, the parameters of the cavity decay rate, exciton dipole decay rate, and the weak coupling strength may cause the error during the input-output process, so the fidelity and the success probability would be affected by these parameters. In 2011, Kastoryano *et al.* [123] prepared the generation of a maximally entangled state of two atoms in an optical cavity, in which the error can be heralded. In 2012, Li *et al.* [124] proposed a practical scheme for single emitter-single-photon interfacing, the fidelity of which is robust even in the weak coupling regime. In 2016, Li and Deng [14] presented a robust error-rejecting quantum entangling gate based on single-sided QD-cavity system. In this scheme, the fidelity of the entangling gate can reach unit one with a detectable error. In 2017, Li *et al.* [15] presented some high-fidelity quantum circuits for quantum computing on electron spins of QDs embedded in low-Q optical microcavities, in which the fidelities of the quantum gates can, in principle, be robust to imperfections involved in a practical input-output process of a single photon by converting the infidelity into a heralded error. Subsequently, this error-detected method [14, 15] was applied in other tasks of quantum information processing, such as universal hyperparallel photonic quantum gates [29, 31], quantum repeaters [56], and error-detected generation and complete analysis of hyperentangled Bell states for photons [94], and hyperentanglement purification [74].

In this paper, we propose a scheme for the error-detected generation of an N-photon cluster state with the quantum dot (QD) embedded in a single-sided optical microcavity. The basic structure of this scheme is an error-detected controlled-phase gate for the hybrid electron–photon system. In this scheme, the errors during the input–output process in practical condition can be detected, which brings a almost unity fidelity and a high success probability. Our scheme for constructing an error-detected controlled-phase gate and N-photon cluster state can be performed by repeating until success. It shows that our scheme is useful in quantum information process in the future.

2 Error-detected hybrid controlled phase gate

We consider a singly charged self-assembled Ga As or In(Ga) As quantum dot(QD) embedded in a single-sided micropillar cavity as shown in Fig. 1(a). The bottom reflector of this cavity is 100% reflective while the top one is partially reflective, so that light can be coupled into and out of the cavity through the top reflector. The optical transition properties of a singly charged QD are dominated by Pauli's exclusion principle [125], as shown in Fig. 1(b). The optical excited states are the trion states X^- ($|\uparrow\downarrow\Uparrow\rangle$ and $|\downarrow\uparrow\Downarrow\rangle$) consisting of two antiparallel electrons and one hole [126]. $|\uparrow\rangle$ and $|\downarrow\rangle$ represent electron-spin states $|+\frac{1}{2}\rangle$ and $|-\frac{1}{2}\rangle$. $|\Uparrow\rangle$ and $|\Downarrow\rangle$ represent heavy-hole spin states $|+\frac{3}{2}\rangle$ and $|-\frac{3}{2}\rangle$ in the valence band, respectively. If the excess electron-spin state is $|\uparrow\rangle$, only the right-handed circularly polarized photon $|R\rangle$ can be resonantly absorbed to create X^- in the state $|\uparrow\downarrow\Uparrow\rangle$. If the excess electron-spin state is $|\downarrow\rangle$, only the left-handed circularly polarized photon $|L\rangle$ can be resonantly absorbed to create X^- in the state $|\downarrow\uparrow\Downarrow\rangle$. The transitions between states $|\uparrow\downarrow\Uparrow\rangle$ and $|\downarrow\rangle$, $|\downarrow\uparrow\Downarrow\rangle$ and $|\uparrow\rangle$ are dipole forbidden.

The optical property of this QD-cavity system can be obtained by solving the Heisenberg equations of the cavity field operator $\hat{a}$ and the dipole operator $\hat{\sigma}_-$ in the interaction picture as formulated in the standard textbook [127]:

$$\begin{aligned}
\frac{\mathrm{d}\hat{a}}{\mathrm{d}t} &= -\left[\mathrm{i}(\omega_c-\omega)+\frac{\kappa}{2}+\frac{\kappa_s}{2}\right]\hat{a}-g\hat{\sigma}_- -\sqrt{\kappa}\hat{a}_{in},\\
\frac{\mathrm{d}\hat{\sigma}_-}{\mathrm{d}t} &= -\left[\mathrm{i}(\omega_{X^-}-\omega)+\frac{\gamma}{2}\right]\hat{\sigma}_- - g\hat{\sigma}_z\hat{a},\\
\hat{a}_{out} &= \hat{a}_{in}+\sqrt{\kappa}\hat{a}, \qquad (1)
\end{aligned}$$

where ω_c, ω and ω_{X^-} describe the frequencies of the cavity

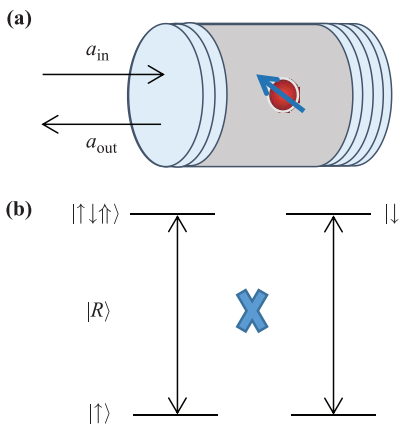


Fig. 1 **(a)** Schematic diagram of a singly charged QD inside a single-sided optical micropillar cavity. **(b)** The relative electron spin energy-levels and the optical transitions of a QD.

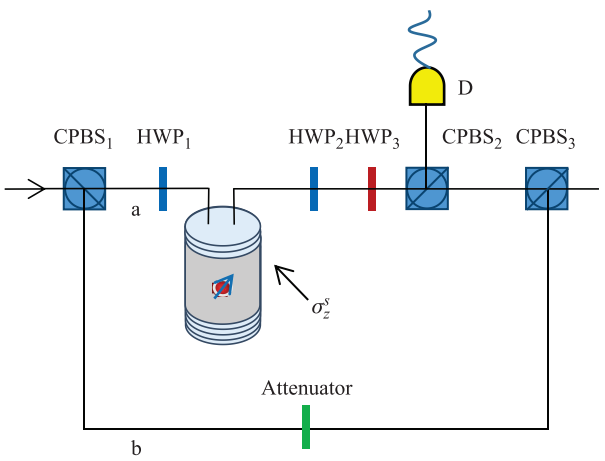


Fig. 2 The schematic setup of the error-detected C-phase gate on the hybrid electron–photon system. CPBS_1, CPBS_2, and CPBS_3 are the circularly polarized beam splitters that transmit $|R\rangle$ photons and reflect $|L\rangle$ photons. HWP_1 and HWP_2 are half-wave plates set at 22.5° to complete the hadamard operation. HWP_3 is set at 45° to flip the state of the circularly polarized photon in the basis of $|R\rangle$ and $|L\rangle$. σ_z^s is to perform the phase-flip operation ($\sigma_z^s = |\uparrow\rangle\langle\uparrow| - |\downarrow\rangle\langle\downarrow|$) on the electron spin. The decay rate of the attenuator is $\frac{(r_1-r_0)}{2}$. D is the photon detector.

mode, the input photon and the trion X^- transition, respectively. g is the coupling strength between the QD and the cavity mode, which vanishes if the cavity mode does not match the trion X^- transition of the QD (so-called empty cavity or cold cavity). $\gamma/2$ is the X^- dipole decay rate, while $\kappa/2$ and $\kappa_s/2$ represent the cavity field decay rates into the input/output modes and the leaky modes (side leakage), respectively. $\hat{a}_{in}$ and $\hat{a}_{out}$ are the input and output field operators. From these equations, one can get the reflection coefficient [120, 121, 128, 129]:

$$r_1(\omega) = \frac{\langle \hat{a}_{out}\rangle}{\langle \hat{a}_{in}\rangle} = 1 - \frac{\kappa[\mathrm{i}(\omega_{X^-} - \omega) + \frac{\gamma}{2}]}{[\mathrm{i}(\omega_{X^-} - \omega) + \frac{\gamma}{2}][\mathrm{i}(\omega_c - \omega) + \frac{\kappa}{2} + \frac{\kappa_s}{2}] + g^2}. \quad (2)$$

For $g = 0$, the reflection coefficient reduces to

$$r_0(\omega) = \frac{\mathrm{i}(\omega_c - \omega) - \frac{\kappa}{2} + \frac{\kappa_s}{2}}{\mathrm{i}(\omega_c - \omega) + \frac{\kappa}{2} + \frac{\kappa_s}{2}}. \quad (3)$$

Suppose initially the excess electron-spin state is $|\varphi_s\rangle = \frac{1}{\sqrt{2}}(|\uparrow\rangle + |\downarrow\rangle)$, while the input photon lies in the superposition of the circularly polarized state $|\varphi_p\rangle = \frac{1}{\sqrt{2}}(|R\rangle + |L\rangle)$. After the photon is reflected by the QD-cavity, the system composed of the photon and the excess electron spin evolves to the state

$$|\Phi\rangle = \frac{1}{2}[(r_1|\uparrow\rangle + r_0|\downarrow\rangle) \otimes |R\rangle + (r_0|\uparrow\rangle + r_1|\downarrow\rangle) \otimes |L\rangle]. \quad (4)$$

With the interaction process described above, we can construct an error-detected C-phase gate on the hybrid electron-photon system, as shown in Fig. 2. It contains a QD-cavity, three CPBSs (circularly polarized beam splitters) which transmit $|R\rangle$ polarization of photons and reflect $|L\rangle$ polarization of photons, a single-photon detector D, an attenuator whose decay rate is $\frac{r_1-r_0}{2}$ and three HWPs (half-wave plates). Among these HWPs, HWP_1 and HWP_2 are half-wave plates set at 22.5° to complete the hadamard operation. HWP_3 is set at 45° to flip the state of the circularly polarized photon. Suppose the input photon state is $|\varphi_p\rangle = \frac{1}{\sqrt{2}}(|R\rangle + |L\rangle)$, while the electron spin state is $|\varphi_s\rangle = \frac{1}{\sqrt{2}}(|\uparrow\rangle + |\downarrow\rangle)$. After the photon passes through the CPBS_1 (which divides the photon into two paths a, b) and HWP_1 [which performs the hadamard operation $|R\rangle \to \frac{1}{\sqrt{2}}(|R\rangle + |L\rangle), |L\rangle \to \frac{1}{\sqrt{2}}(|R\rangle - |L\rangle)$], the state of the system composed of the QD and the input photon evolves into

$$|\Phi\rangle_1 = \frac{1}{2}(|\uparrow\rangle + |\downarrow\rangle) \otimes \left[\frac{1}{\sqrt{2}}(|R_a\rangle + |L_a\rangle) + |L_b\rangle\right]. \quad (5)$$

Here $|R_a\rangle$ and $|L_a\rangle$ denote the $|R\rangle$ and $|L\rangle$ polarizations of a photon through path a which is generated from $|R\rangle$ polarization of the photon by HWP_1, while $|L_b\rangle$ denotes the reflected component of the photon from CPBS_1 through path b. After the photon interacts with the QD-cavity, the state of the system composed of the QD and the input photon changes to

$$|\Phi\rangle_2 = \frac{1}{2}\left[\frac{1}{\sqrt{2}}(r_1|\uparrow\rangle + r_0|\downarrow\rangle) \otimes |R_a\rangle + \frac{1}{\sqrt{2}}(r_0|\uparrow\rangle + r_1|\downarrow\rangle) \otimes |L_a\rangle + (|\uparrow\rangle + |\downarrow\rangle) \otimes |L_b\rangle\right]. \quad (6)$$

Let the photon pass through HWP_2, which applies the hadamard operation on the photon, then the state of the hybrid electron-photon system evolves into

$$|\Phi\rangle_3 = \frac{1}{2}\left[\frac{1}{\sqrt{2}} \cdot \frac{1}{\sqrt{2}}(r_1|\uparrow\rangle + r_0|\downarrow\rangle)(|R_a\rangle + |L_a\rangle) + \frac{1}{\sqrt{2}} \cdot \frac{1}{\sqrt{2}}(r_0|\uparrow\rangle + r_1|\downarrow\rangle)(|R_a\rangle - |L_a\rangle) + (|\uparrow\rangle + |\downarrow\rangle) \otimes |L_b\rangle\right]$$
$$= \frac{1}{2}\left[\frac{1}{2}(r_1 + r_0)(|\uparrow\rangle + |\downarrow\rangle) \otimes |R_a\rangle + \frac{1}{2}(r_1 - r_0)(|\uparrow\rangle - |\downarrow\rangle) \otimes |L_a\rangle + (|\uparrow\rangle + |\downarrow\rangle) \otimes |L_b\rangle\right]. \quad (7)$$

After the photon passes through HWP_3 which performs the bit-flip operator $\hat{X} = |R\rangle\langle L| + |L\rangle\langle R|$ on the photon, the state of the hybrid electron–photon system becomes

$$|\Phi\rangle_4 = \frac{1}{2}\Big[\frac{1}{2}(r_1 + r_0)(|\uparrow\rangle + |\downarrow\rangle) \otimes |L_a\rangle + \frac{1}{2}(r_1 - r_0)(|\uparrow\rangle - |\downarrow\rangle) \otimes |R_a\rangle + (|\uparrow\rangle + |\downarrow\rangle) \otimes |L_b\rangle\Big]. \tag{8}$$

Then let $|L_b\rangle$ pass through the attenuator whose decay rate is $\frac{r_1 - r_0}{2}$. In the mean time, $|L_a\rangle$ will be reflected by CPBS_2. After that, the state of the hybrid electron-photon system evolves into

$$|\Phi\rangle_5 = \frac{(r_1 - r_0)}{4}[(|\uparrow\rangle + |\downarrow\rangle) \otimes |L_b\rangle + (|\uparrow\rangle - |\downarrow\rangle) \otimes |R_a\rangle] + \frac{(r_1 + r_0)}{4}(|\uparrow\rangle + |\downarrow\rangle) \otimes |L_a\rangle. \tag{9}$$

If the photon passes through CPBS_3 without being detected by photon detector D, a single-qubit operation $\hat{\sigma}_z^s$ ($\hat{\sigma}_z^s = |\uparrow\rangle\langle\uparrow| - |\downarrow\rangle\langle\downarrow|$) on the electron spin will evolve the system into

$$\begin{aligned}|\Phi\rangle_6 &= \frac{r_1 - r_0}{4}[(|\uparrow\rangle - |\downarrow\rangle) \otimes |L\rangle + (|\uparrow\rangle + |\downarrow\rangle) \otimes |R\rangle] \\ &= \frac{r_1 - r_0}{4}[|\uparrow\rangle|L\rangle - |\downarrow\rangle|L\rangle + |\uparrow\rangle|R\rangle + |\downarrow\rangle|R\rangle] \\ &= \frac{r_1 - r_0}{4}[(|\uparrow\rangle + |\downarrow\rangle\hat{\sigma}_z^p) \otimes (|R\rangle + |L\rangle)].\end{aligned} \tag{10}$$

Here $\hat{\sigma}_z^p = |R\rangle\langle R| - |L\rangle\langle L|$. If the photon detector clicks, the state of the hybrid electron-photon system will project to $|\Phi\rangle_6' = \frac{r_1 + r_0}{4}(|\uparrow\rangle + |\downarrow\rangle) \otimes |L_a\rangle$.

The Eq. (10) represents an error-detected C-phase gate on the hybrid electron-photon system with the electron as a controlling qubit while the photon as the targeting qubit. $|L_a\rangle$ in the last term on the right-hand side of Eq. (9) ($|\Phi\rangle_6'$) is the left-handed polarization component which passed through the QD-cavity and triggered a click on a photon detector. The detection of the $|L_a\rangle$ signals an error caused by the unbalance of the two reflection coefficients r_1 and r_0 that may originate from the low-Q cavity (or the mismatch between the incident photon field and the cavity mode). Fortunately, under this circumstance, the state of the electron spin is the same as the original state as if there was no interaction with the photon. If the C-phase gate fails, one can input another photon to repeat above process until the single photon detector D will not click.

3 N-photon cluster state generation

With the help of error-detected hybrid controlled phase gate, one can get an N-photon cluster state with high fidelity. A cluster state is a multipartite entangled state which has special features suitable for implementing a quantum computer on a network, and it is first defined by Briegel and Raussendorf [96] in 2001. An N-photon cluster state is defined as $|\Phi\rangle = (|R_N\rangle + |L_N\rangle \cdot \hat{\sigma}_z^{p,N-1}) \otimes (|R_{N-1}\rangle + |L_{N-1}\rangle \cdot \hat{\sigma}_z^{p,N-2}) \ldots \otimes (|R_1\rangle + |L_1\rangle)$. The schematic diagram of our error-detected N-photon cluster state generation is shown in Fig. 3, which consists of the error-detected C-phase gate and a HWP (half-wave plate). The electron spin lies in the state $\frac{1}{\sqrt{2}}(|\uparrow\rangle + |\downarrow\rangle)$. The N photons with the same frequency are initially in the linear polarized state $\frac{1}{\sqrt{2}}(|R_i\rangle + |L_i\rangle)$ (here $i = 1, 2, \ldots, N$), respectively. They are injected in sequence into the QD-cavity. The time interval between two photons is Δt, which is required to be less than the electron spin coherence time. The detailed process to generate N-photon cluster state is described as follows.

When the first photon passes through the error-detected C-phase gate block until CPBS_3 without being detected by photon detector D, the state of the hybrid electron-photon system becomes

$$|\Phi\rangle_7 = \frac{r_1 - r_0}{4}[(|\uparrow\rangle + |\downarrow\rangle\hat{\sigma}_z^{p,1}) \otimes (|R_1\rangle + |L_1\rangle)]. \tag{11}$$

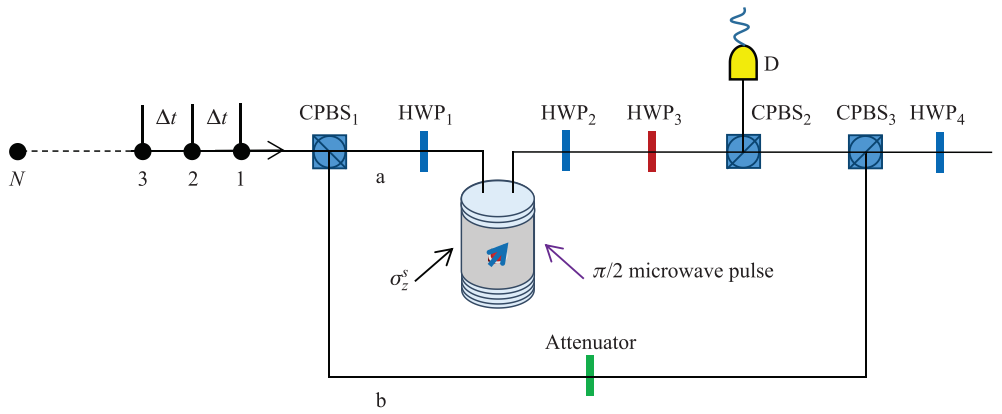


Fig. 3 The setup for generating the error-detected N-photon cluster state. HWP_1, HWP_2, HWP_4 are half-wave plates set at 22.5° to complete the hadamard operation. HWP_3 is set at 45° to flip the state of the circularly polarized photon. $\pi/2$ microwave pulse is to complete hadamard operation on the electron spin.

Then the second photon is put into the setup. After it is reflected by the QD-cavity and passes through these linear optical elements until $CPBS_3$ without being detected by photon detector D, the output state of the system contains two photons and one electron changes to

$$|\Phi\rangle_8 = \frac{1}{\sqrt{2}} \cdot \left(\frac{r_1 - r_0}{2\sqrt{2}}\right)^2 [|\uparrow\rangle \otimes (|R_2\rangle + |L_2\rangle) \otimes (|R_1\rangle + |L_1\rangle) + |\downarrow\rangle \otimes ((|R_2\rangle - |L_2\rangle) \otimes \hat{\sigma}_z^{p,1}(|R_1\rangle + |L_1\rangle)]. \quad (12)$$

After the second photon passes through the HWP_4 which performs the hadamard operation on this photon, a $\pi/2$ microwave pulse is added on the electron spin which performs a hadamard operation $[|\uparrow\rangle \to \frac{1}{\sqrt{2}}(|\uparrow\rangle + |\downarrow\rangle), |\downarrow\rangle \to \frac{1}{\sqrt{2}}(|\uparrow\rangle - |\downarrow\rangle)]$ on the electron, and the state of the system contains two photons and one electron becomes

$$|\Phi\rangle_9 = \frac{1}{\sqrt{2}} \cdot \left(\frac{r_1 - r_0}{2\sqrt{2}}\right)^2 [(|\uparrow\rangle + |\downarrow\rangle\hat{\sigma}_z^{p,2}) \otimes (|R_2\rangle + |L_2\rangle\hat{\sigma}_z^{p,1}) \otimes (|R_1\rangle + |L_1\rangle)]. \quad (13)$$

Here the term on the right-handed side of the Eq. (13) contains two C-phase gates. One is the C-phase gate on the hybrid electron-photon system, and another one is the C-phase gate between two photons. If there is a click on photon detector D during the second photon passing through the setup, the system state will project to

$$|\Phi\rangle_9' = \frac{1}{\sqrt{2}} \cdot \frac{(r_1 - r_0)(r_1 + r_0)}{(2\sqrt{2})^2} [(|\uparrow\rangle + |\downarrow\rangle\hat{\sigma}_z^{p,1}) \otimes |L_{2a}\rangle \otimes (|R_1\rangle + |L_1\rangle)] \quad (14)$$

The click of the photon detector D signals there is an error during the interaction between the second photon and the electron. After the detection on the second photon, the state of the system contains the first photon and the electron will be projected to the state in Eq. (11), so one can put another photon as the second one into this setup without initiating the electron-spin state.

The remaining photons are injected into the setup and repeat the above process as shown in Fig. 3. After the N photons pass through the setup shown in Fig. 3, if there is no click on the photon detector D, the state of the system contains N photons and one electron becomes

$$\begin{aligned}|\Phi\rangle_{10} = {} & \frac{1}{\sqrt{2}} \cdot \left(\frac{r_1 - r_0}{2\sqrt{2}}\right)^N |\uparrow\rangle[(|R_N\rangle + |L_N\rangle \cdot \hat{\sigma}_z^{p,N-1}) \\ & \otimes (|R_{N-1}\rangle + |L_{N-1}\rangle \cdot \hat{\sigma}_z^{p,N-2}) \ldots \otimes (|R_1\rangle + |L_1\rangle)] \\ & + \frac{1}{\sqrt{2}} \cdot \left(\frac{r_1 - r_0}{2\sqrt{2}}\right)^N |\downarrow\rangle[(|R_N\rangle - |L_N\rangle\hat{\sigma}_z^{p,N-1}) \\ & \otimes (|R_{N-1}\rangle + |L_{N-1}\rangle\hat{\sigma}_z^{p,N-2}) \ldots \otimes (|R_1\rangle + |L_1\rangle)]. \end{aligned} \quad (15)$$

Then one can obtain the N-photon cluster state from above equation by measuring the electron spin state in two orthogonal bases $(|\uparrow\rangle, |\downarrow\rangle)$. If the electron spin state lies in the state $|\uparrow\rangle$, the N-photon state will collapse to

$$\begin{aligned}|\psi_N\rangle = {} & \left(\frac{r_1 - r_0}{2\sqrt{2}}\right)^N [(|R_N\rangle + |L_N\rangle \cdot \hat{\sigma}_z^{p,N-1}) \\ & \otimes (|R_{N-1}\rangle + |L_{N-1}\rangle \cdot \hat{\sigma}_z^{p,N-2}) \ldots \otimes (|R_1\rangle + |L_1\rangle)]. \end{aligned} \quad (16)$$

If the measurement result is $|\downarrow\rangle$, the N-photon state can be written as

$$\begin{aligned}|\psi_N'\rangle = {} & \left(\frac{r_1 - r_0}{2\sqrt{2}}\right)^N [(|R_N\rangle - |L_N\rangle \cdot \hat{\sigma}_z^{p,N-1}) \\ & \otimes (|R_{N-1}\rangle + |L_{N-1}\rangle \cdot \hat{\sigma}_z^{p,N-2}) \ldots \otimes (|R_1\rangle + |L_1\rangle)]. \end{aligned} \quad (17)$$

For the latter situation in Eq. (17), one can perform a single-qubit operation $\hat{\sigma}_z$ (the phase-flip operation $\hat{\sigma}_z = |R\rangle\langle R| - |L\rangle\langle L|$) on the Nth photon. This phase-flip operation can be achieved with 3 HWPs, two of which are set at 22.5° to perform a hadamard operation on the photon, while the last one is set at 45° to perform a bit-flip operation $X = |R\rangle\langle L| + |L\rangle\langle R|$ on the photon. Then the above state $|\psi_N'\rangle$ can be changed to the state $|\psi_N\rangle$, which is the result aimed to achieve. If the photon detector D clicks during above process, the system state will project into

$$\begin{aligned}|\Phi\rangle_{11} = {} & \frac{1}{\sqrt{2}} \cdot \frac{r_1 + r_0}{2\sqrt{2}} \left(\frac{r_1 - r_0}{2\sqrt{2}}\right)^{j-1} (|\uparrow\rangle + |\downarrow\rangle) \\ & \otimes |L_{ja}\rangle \otimes (|R_{j-1}\rangle + |L_{j-1}\rangle \cdot \hat{\sigma}_z^{p,j-2}) \\ & \otimes (|R_{j-2}\rangle + |L_{j-2}\rangle \cdot \hat{\sigma}_z^{p,j-3}) \otimes \ldots (|R_1\rangle + |L_1\rangle), \end{aligned} \quad (18)$$

here $j \in N$.

Eq. (16) describes an N-photon cluster state. With this scheme, one can get an N-photon cluster state no matter which state the electron state is measured on. While the Eq. (18) ($|\Phi\rangle_{11}$) contains $|L_{ja}\rangle$ which is the left-handed polarization component passed through the QD-cavity. It leads to click on the photon detector D which means there are errors during the interaction between the photon and the electron. In this condition, one can put another photon which lies in the state $\frac{1}{\sqrt{2}}(|R\rangle + |L\rangle)$ to repeat the above process until the cluster state is generated successfully.

4 Discussion and summary

The fidelity for the generation of N-photon cluster state is defined as $F = |\langle\psi_r|\psi_i\rangle|^2$. $|\psi_i\rangle$ and $|\psi_r\rangle$ are the final states in the ideal condition and realistic condition, respectively. In our scheme, the N-photon cluster state generation can be achieved with the unity fidelity in both the ideal condition and the realistic condition. Therefore, the fidelity is independent of the side leakage κ_s/κ, the

detuning $(\omega_c - \omega)/\kappa$, the number of photons N, and the cooperativity $C \equiv g^2/\kappa_T$, here $\kappa_T = \kappa_s + \kappa$. It benefits from our error-detected procedure. Specifically, when there are errors caused by imperfect input-output process, these errors can be detected by photon detector D without affecting the output state. The output state means the the state of the system contains N photons without detected and one electron in the QD cavity. That means the fidelity is not affected by these errors caused by realistic input-output process such as the cavity decay, nonzero bandwidth, photon loss, and the finite coupling, which is far different from other schemes for generating cluster state [130]. If the photon detector D clicks, one can input another photon to repeat the process without reinitialization of the QD since the electron spin still lies in the initial states.

In our scheme, the probability to get the N-photon cluster state successfully is

$$\eta_s = \left(\frac{r_1 - r_0}{2}\right)^{2N}. \tag{19}$$

While the heralded error probability of this scheme is

$$\eta_e = \sum_{j=1}^{N} \frac{(r_1 + r_0)^2}{8} \left(\frac{r_1 - r_0}{2}\right)^{2j-2}. \tag{20}$$

In this case, the electron spin can be directly used in the recycling procedure. By taking the recycling procedure into account, the success probability η of our error-rejecting N-photon cluster state is defined as

$$\eta = \frac{\eta_s}{1 - \eta_e}. \tag{21}$$

The success probability of above N-photon cluster state varies with the side leakage κ_s/κ, the error rate of the detuning $(\omega_c - \omega)/\kappa$, the number of photons N and the cooperativity $C \equiv \mathrm{g}^2/\gamma\kappa_T$, here $\kappa_T = \kappa_s + \kappa$, as shown in Fig. 4. In the ideal condition when the QD is strongly coupled to the cavity, $C \gg 1$. For the low-Q cavity (resonantly scattering regime), the typical value of C is 1/4. Here we let the cooperativity $C = 1$ as a normal value of the Purcell regime. We set $\gamma/\kappa = 0.1$ where γ is typically $\ll 0.1\kappa$ for most QD-cavity experiments [131–133]. As for the spin coherent time, it can reach 0.44 μs in GaAs QDs, which is much longer than the time scale for generating entanglement [134], so the error-detected cluster state generation scheme can work many times before the decoherence time. And we let the number of photon N be 2 (black solid line), 3 (red dotted line) and 4 (blue dashed line), respectively. Figure 4 shows that the success probability decreases as the side leakage κ_s/κ and the particle number N increasing. When the detuning $(\omega_c - \omega)/\kappa = 0.1$, the success probability to get the 3-photon cluster state can reach about 0.24. When the detuning $(\omega_c - \omega)/\kappa = 0$, the success probability to get the 3-photon cluster state can get 0.27.

The total success probability of our N-photon cluster state generation scheme is affected by error items during practical input–output process. Luckily, error items lead to clicks on the photon detector D, which signal the restart of our setup. By repeating interaction procedure until cluster state is prepared successfully, the success probability can be improved largely especially in weak coupling situation. More than that, our scheme only use single-sided optical microcavities, which only have unilateral input–output processes. Compared with other existing double-sided QD-cavity systems or other physical systems [130, 135], our scheme has a higher success probability.

In summary, we have proposed a scheme for generating an N-photon cluster state with error-detected method. The basic structure of this scheme is an error-detected controlled-phase gate for the hybrid electron-photon system. Our scheme considers the errors that may occur during the interaction process, and these errors lead to a click on the photon detector. It results a higher success probability compared with the other existing schemes by introducing the recycling procedure. More than that, when there are errors, the electron spin state has been

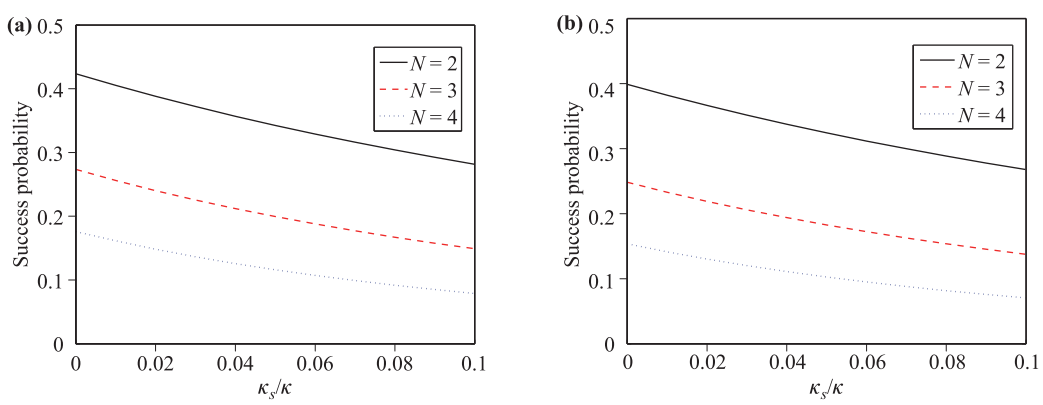


Fig. 4 The success probability of N-photon cluster state vs. κ_s/κ, here $\omega_{X^-} = \omega$, $C = 1$ and $\gamma/\kappa = 0.1$. **(a)** $(\omega_c - \omega)/\kappa = 0$, **(b)** $(\omega_c - \omega)/\kappa = 0.1$. The black solid line, the red dotted line, and the blue dashed line describe the performance of our scheme for generating 2-photon, 3-photon, 4-photon cluster state, respectively.

not changed, one can put another photon without initialize the electron of the QD-cavity. These advantages make our schemes for generating N-photon cluster state more useful in the quantum computation and quantum network in the future.

Acknowledgements This work was supported by the National Natural Science Foundation of China under Grant No. 11475021 and the National Key Basic Research Program of China under Grant No. 2013CB922000. We thank F. G. Deng and B. C. Ren for their useful discussions.

References

1. M. A. Nielsen and I. L. Chuang, Quantum Computation and Quantum Information, Cambridge: Cambridge University Press, 2000
2. P. W. Shor, Algorithms for quantum computation: discrete logarithms and factoring, in: Proceedings of the 35th Annual Symposium on Foundations of Computer Science, S. Goldwasser, pp 124–134, IEEE Computer Society Press, 1994
3. L. K. Grover, Quantum mechanics helps in searching for a needle in a haystack, *Phys. Rev. Lett.* 79(2), 325 (1997)
4. G. L. Long, Grover algorithm with zero theoretical failure rate, *Phys. Rev. A* 64(2), 022307 (2001)
5. Y. B. Sheng and L. Zhou, Blind quantum computation with a noise channel, *Phys. Rev. A* 98(5), 052343 (2018)
6. Z. Z. Zou, X. T. Yu, and Z. C. Zhang, Quantum connectivity optimization algorithms for entanglement source deployment in a quantum multi-hop network, *Front. Phys.* 13(2), 130202 (2018)
7. N. A. Gershenfeld and I. L. Chuang, Bulk spin-resonance quantum computation, *Science* 275(5298), 350 (1997)
8. G. R. Feng, G. F. Xu, and G. L. Long, Experimental realization of nonadiabatic holonomic quantum computation, *Phys. Rev. Lett.* 110(19), 190501 (2013)
9. Y. Long, G. R. Feng, Y. C. Tang, W. Qin, and G. L. Long, NMR realization of adiabatic quantum algorithms for the modified Simon problem, *Phys. Rev. A* 88(1), 012306 (2013)
10. X. K. Song, H. Zhang, Q. Ai, J. Qiu, and F. G. Deng, Shortcut to adiabatic holonomic quantum computation in decoherence-free subspace with transitionless quantum driving algorithm, *New J. Phys.* 18(2), 023001 (2016)
11. X. K. Song, Q. Ai, J. Qiu, and F. G. Deng, Physically feasible three-level transitionless quantum driving with multiple Schrödinger dynamics, *Phys. Rev. A* 93(5), 052324 (2016)
12. D. Loss and D. P. DiVincenzo, Quantum computation with quantum dots, *Phys. Rev. A* 57(1), 120 (1998)
13. A. Imamoglu, D. D. Awschalom, G. Burkard, D. P. DiVincenzo, D. Loss, M. Sherwin, and A. Small, Quantum information processing using quantum dot spins and cavity QED, *Phys. Rev. Lett.* 83(20), 4204 (1999)
14. T. Li and F. G. Deng, Error-rejecting quantum computing with solid-state spins assisted by low-Q optical microcavities, *Phys. Rev. A* 94(6), 062310 (2016)
15. T. Li, J. C. Gao, F. G. Deng, and G. L. Long, High-fidelity quantum gates on quantum-dot-confined electron spins in low-Q optical microcavities, *Ann. Phys.* 391, 150 (2018)
16. T. van der Sar, Z. H. Wang, M. S. Blok, H. Bernien, T. H. Taminiau, D. M. Toyli, D. A. Lidar, D. D. Awschalom, R. Hanson, and V. V. Dobrovitski, Decoherence-protected quantum gates for a hybrid solid-state spin register, *Nature* 484(7392), 82 (2012)
17. H. R. Wei and F. G. Deng, Compact quantum gates on electron-spin qubits assisted by diamond nitrogen-vacancy centers inside cavities, *Phys. Rev. A* 88(4), 042323 (2013)
18. T. Yamamoto, Y. A. Pashkin, O. Astafiev, Y. Nakamura, and J. S. Tsai, Demonstration of conditional gate operation using superconducting charge qubits, *Nature* 425(6961), 941 (2003)
19. M. Hua, M. J. Tao, A. Alsaedi, T. Hayat, and F. G. Deng, Universal distributed quantum computing on superconducting qutrits with dark photons, *Ann. Phys.* 530(4), 1700402 (2018)
20. H. Fan and X. B. Zhu, superconducting qubits for quantum walks, *Front. Phys.* 14(6), 61201 (2019)
21. X. Li, Y. Wu, D. Steel, D. Gammon, T. H. Stievater, D. S. Katzer, D. Park, C. Piermarocchi, and L. J. Sham, An all-optical quantum gate in a semiconductor quantum dot, *Science* 301(5634), 809 (2003)
22. E. Knill, R. Laflamme, and G. J. Milburn, A scheme for efficient quantum computation with linear optics, *Nature* 409(6816), 46 (2001)
23. M. A. Nielsen, Optical quantum computation using cluster states, *Phys. Rev. Lett.* 93(4), 040503 (2004)
24. H. R. Wei and F. G. Deng, Scalable photonic quantum computing assisted by quantum-dot spin in double-sided optical microcavity, *Opt. Express* 21(15), 17671 (2013)
25. C. Wang, Y. Zhang, R. Z. Jiao, and G. S. Jin, Universal quantum controlled phase gate on photonic qubits based on nitrogen vacancy centers and microcavity resonators, *Opt. Express* 21(16), 19252 (2013)
26. Y. H. Kang, Y. Xia, and P. M. Lu, Two-photon phase gate with linear optical elements and atom-cavity system, *Quantum Inform. Process.* 15(11), 4521 (2016)
27. B. C. Ren and F. G. Deng, Hyper-parallel photonic quantum computing with coupled quantum dots, *Sci. Rep.* 4(1), 4623 (2015)
28. B. C. Ren, G. Y. Wang, and F. G. Deng, Universal hyperparallel hybrid photonic quantum gates with dipole-induced transparency in the weak-coupling regime, *Phys. Rev. A* 91(3), 032328 (2015)
29. B. C. Ren, and F. G. Deng, Robust hyperparallel photonic quantum entangling gate with cavity QED, *Opt. Express* 25(10), 10863 (2017)

30. T. Li and G. L. Long, Hyperparallel optical quantum computation assisted by atomic ensembles embedded in double-sided optical cavities, *Phys. Rev. A* 94(2), 022343 (2016)

31. G. Y. Wang, T. Li, Q. Ai, and F. G. Deng, Self-error-corrected hyperparallel photonic quantum computation working with both the polarization and the spatial-mode degrees of freedom, *Opt. Express* 26(18), 23333 (2018)

32. B. C. Ren, A. H. Wang, A. Alsaedi, T. Hayat, and F. G. Deng, Three-photon polarization-spatial hyperparallel quantum Fredkin gate assisted by diamond nitrogen vacancy center in optical cavity, *Ann. Phys.* 530(5), 1800043 (2018)

33. F. G. Deng, B. C. Ren, and X. H. Li, Quantum hyperentanglement and its applications in quantum information processing, *Sci. Bull.* 62(1), 46 (2017)

34. D. Jaksch, H. J. Briegel, J. I. Cirac, C. W. Gardiner, and P. Zoller, Entanglement of atoms via cold controlled collisions, *Phys. Rev. Lett.* 82(9), 1975 (1999)

35. D. Jaksch, J. I. Cirac, P. Zoller, S. L. Rolston, R. Côté, and M. D. Lukin, Fast quantum gates for neutral atoms, *Phys. Rev. Lett.* 85(10), 2208 (2000)

36. G. Z. Song, Q. Liu, J. Qiu, G. J. Yang, F. Alzahrani, A. Hobiny, F. G. Deng, and M. Zhang, Heralded quantum gates for atomic systems assisted by the scattering of photons off single emitters, *Ann. Phys.* 387, 152 (2017)

37. J. Joo and D. L. Feder, Error-correcting one-way quantum computation with global entangling gates, *Phys. Rev. A* 80(3), 032312 (2009)

38. A. K. Ekert, Quantum cryptography based on Bell's theorem, *Phys. Rev. Lett.* 67(6), 661 (1991)

39. C. H. Bennett, G. Brassard, and N. D. Mermin, Quantum cryptography without Bell's theorem, *Phys. Rev. Lett.* 68(5), 557 (1992)

40. X. H. Li, F. G. Deng, and H. Y. Zhou, Efficient quantum key distribution over a collective noise channel, *Phys. Rev. A* 78(2), 022321 (2008)

41. M. Hillery, V. Bužek, and A. Berthiaume, Quantum secret sharing, *Phys. Rev. A* 59(3), 1829 (1999)

42. G. L. Long and X. S. Liu, Theoretically efficient high-capacity quantum-key-distribution scheme, *Phys. Rev. A* 65(3), 032302 (2002)

43. F. G. Deng, G. L. Long, and X. S. Liu, Two-step quantum direct communication protocol using the Einstein–Podolsky–Rosen pair block, *Phys. Rev. A* 68(4), 042317 (2003)

44. F. Z. Wu, G. J. Yang, H. B. Wang, J. Xiong, F. Alzahrani, A. Hobiny, and F. G. Deng, High-capacity quantum secure direct communication with two-photon six-qubit hyperentangled states, *Sci. China Phys. Mech. Astron.* 60(12), 120313 (2017)

45. W. Zhang, D. S. Ding, Y. B. Sheng, L. Zhou, B. S. Shi, and G. C. Guo, Quantum secure direct communication with quantum memory, *Phys. Rev. Lett.* 118(22), 220501 (2017)

46. F. Zhu, W. Zhang, Y. B. Sheng, and Y. D. Huang, Experimental long-distance quantum secure direct communication, *Sci. Bull.* 62(22), 1519 (2017)

47. S. S. Chen, L. Zhou, W. Zhong, and Y. B. Sheng, Three-step three-party quantum secure direct communication, *Sci. China Phys. Mech. Astron.* 61, 090312 (2017)

48. C. H. Bennett, G. Brassard, C. Crepeau, R. Jozsa, A. Peres, and W. K. Wootters, Teleporting an unknown quantum state via dual classical and Einstein–Podolsky–Rosen channels, *Phys. Rev. Lett.* 70(13), 1895 (1993)

49. C. H. Bennett and S. J. Wiesner, Communication via one- and two-particle operators on Einstein–Podolsky–Rosen states, *Phys. Rev. Lett.* 69(20), 2881 (1992)

50. X. S. Liu, G. L. Long, D. M. Tong, and F. Li, General scheme for superdense coding between multiparties, *Phys. Rev. A* 65(2), 022304 (2002)

51. H. J. Briegel, W. Dur, J. I. Cirac, and P. Zoller, Quantum repeaters:the role of imperfect local operations in quantum communication, *Phys. Rev. Lett.* 81(26), 5932 (1998)

52. L. M. Duan, M. D. Lukin, J. I. Cirac, and P. Zoller, Long-distance quantum communication with atomic ensembles and linear optics, *Nature* 414(6862), 413 (2001)

53. N. Sangouard, C. Simon, H. de Riedmatten, and N. Gisin, Quantum repeaters based on atomic ensembles and linear optics, *Rev. Mod. Phys.* 83(1), 33 (2011)

54. T. J. Wang, S. Y. Song, and G. L. Long, Quantum repeater based on spatial entanglement of photons and quantum-dot spins in optical microcavities, *Phys. Rev. A* 85(6), 062311 (2012)

55. T. Li, G. J. Yang, and F. G. Deng, Heralded quantum repeater for a quantum communication network based on quantum dots embedded in optical microcavities, *Phys. Rev. A* 93(1), 012302 (2016)

56. G. Z. Song, M. Zhang, Q. Ai, G. J. Yang, A. Alsaedi, A. Hobiny, and F. G. Deng, Heralded quantum repeater based on the scattering of photons off single emitters in one-dimensional waveguides, *Ann. Phys.* 378, 33 (2017)

57. P. G. Kwiat, E. Waks, A. G. White, I. Appelbaum, and P. H. Eberhard, Ultrabright source of polarization-entangled photons, *Phys. Rev. A* 60(2), R773 (1999)

58. J. T. Barreiro, N. K. Langford, N. A. Peters, and P. G. Kwiat, Generation of hyperentangled photon pairs, *Phys. Rev. Lett.* 95(26), 260501 (2005)

59. R. Ceccarelli, G. Vallone, F. De Martini, P. Mataloni, and A. Cabello, Experimental entanglement and nonlocality of a two-photon six-qubit cluster state, *Phys. Rev. Lett.* 103(16), 160401 (2009)

60. D. Kalamidas, Linear optical scheme for error-free entanglement distribution and a quantum repeater, *Phys. Rev. A* 73(5), 054304 (2006)

61. T. Yamamoto, J. Shimamura, S. K. Ozdemir, M. Koashi, and N. Imoto, Faithful qubit distribution assisted by one additional qubit against collective noise, *Phys. Rev. Lett.* 95(4), 040503 (2005)

62. X. H. Li, F. G. Deng, and H. Y. Zhou, Faithful qubit transmission against collective noise without ancillary qubits, *Appl. Phys. Lett.* 91(14), 144101 (2007)
63. C. Y. Gao, G. Y. Wang, H. Zhang, and F. G. Deng, Multi-photon self-error-correction hyperentanglement distribution over arbitrary collective-noise channels, *Quantum Inform. Process.* 16(1), 11 (2017)
64. Y. X. Jiang, P. L. Guo, C. Y. Gao, H. B. Wang, F. Alzahrani, A. Hobiny, and F. G. Deng, Self-error-rejecting photonic qubit transmission in polarization-spatial modes with linear optical elements, *Sci. China Phys. Mech. Astron.* 60(12), 120312 (2017)
65. C. H. Bennett, G. Brassard, S. Popescu, B. J. Schumacher, A. Smolin, and W. K. Wootters, Purification of noisy entanglement and faithful teleportation via noisy channels, *Phys. Rev. Lett.* 76(5), 722 (1996)
66. C. Simon and J. W. Pan, Polarization entanglement purification using spatial entanglement, *Phys. Rev. Lett.* 89(25), 257901 (2002)
67. Y. B. Sheng and F. G. Deng, Deterministic entanglement purification and complete nonlocal Bell-state analysis with hyperentanglement, *Phys. Rev. A* 81(3), 032307 (2010)
68. Y. B. Sheng and F. G. Deng, One-step deterministic polarization-entanglement purification using spatial entanglement, *Phys. Rev. A* 82(4), 044305 (2010)
69. X. H. Li, Deterministic polarization-entanglement purification using spatial entanglement, *Phys. Rev. A* 82(4), 044304 (2010)
70. F. G. Deng, One-step error correction for multipartite polarization entanglement, *Phys. Rev. A* 83(6), 062316 (2011)
71. Y. B. Sheng and L. Zhou, Deterministic polarization entanglement purification using time-bin entanglement, *Laser Phys. Lett.* 11(8), 085203 (2014)
72. B. C. Ren, F. F. Du, and F. G. Deng, Two-step hyperentanglement purification with the quantum-state-joining method, *Phys. Rev. A* 90(5), 052309 (2014)
73. G. Y. Wang, Q. Liu, and F. G. Deng, Hyperentanglement purification for two-photon six-qubit quantum systems, *Phys. Rev. A* 94(3), 032319 (2016)
74. G. Y. Wang, T. Li, Q. Ai, A. Alsaedi, T. Hayat, and F. G. Deng, Heralded entanglement purification for high-capacity quantum communication with two-photon four-qubit systems, arXiv: 1802.00111 (2018)
75. L. Zhou and Y. B. Sheng, Polarization entanglement purification for concatenated Greenberger–Horne–Zeilinger state, *Ann. Phys.* 385, 10 (2017)
76. L. Zhou and Y. B. Sheng, Purification of Logic-Qubit Entanglement, *Sci. Rep.* 6(1), 28813 (2016)
77. C. H. Bennett, H. J. Bernstein, S. Popescu, and B. Schumacher, Concentrating partial entanglement by local operations, *Phys. Rev. A* 53(4), 2046 (1996)
78. Z. Zhao, J. W. Pan, and M. S. Zhan, Practical scheme for entanglement concentration, *Phys. Rev. A* 64(1), 014301 (2001)
79. T. Yamamoto, M. Koashi, and N. Imoto, Concentration and purification scheme for two partially entangled photon pairs, *Phys. Rev. A* 64(1), 012304 (2001)
80. Y. B. Sheng, F. G. Deng, and H. Y. Zhou, Nonlocal entanglement concentration scheme for partially entangled multipartite systems with nonlinear optics, *Phys. Rev. A* 77(6), 062325 (2008)
81. B. C. Ren, F. F. Du, and F. G. Deng, Hyperentanglement concentration for two-photon four-qubit systems with linear optics, *Phys. Rev. A* 88(1), 012302 (2013)
82. B. C. Ren and G. L. Long, General hyperentanglement concentration for photon systems assisted by quantum-dot spins inside optical microcavities, *Opt. Express* 22(6), 6547 (2014)
83. X. H. Li and S. Ghose, Hyperentanglement concentration for time-bin and polarization hyperentangled photons, *Phys. Rev. A* 91(6), 062302 (2015)
84. C. Cao, T. J. Wang, S. C. Mi, R. Zhang, and C. Wang, Nonlocal hyperconcentration on entangled photons using photonic module system, *Ann. Phys.* 369, 128 (2016)
85. J. Liu, L. Zhou, W. Zhong, and Y. B. Sheng, Logic Bell state concentration with parity check measurement, *Front. Phys.* 14(2), 21601 (2019)
86. P. G. Kwiat and H. Weinfurter, Embedded Bell-state analysis, *Phys. Rev. A* 58(4), R2623 (1998)
87. N. Lütkenhaus, J. Calsamiglia, and K. A. Suominen, Bell measurements for teleportation, *Phys. Rev. A* 59(5), 3295 (1999)
88. C. Schuck, G. Huber, C. Kurtsiefer, and H. Weinfurter, Complete deterministic linear optics Bell state analysis, *Phys. Rev. Lett.* 96(19), 190501 (2006)
89. T. C. Wei, J. T. Barreiro, and P. G. Kwiat, Hyperentangled Bell state analysis, *Phys. Rev. A* 75(6), 060305 (2007)
90. Y. B. Sheng, F. G. Deng, and G. L. Long, Complete hyperentangled-Bell-state analysis for quantum communication, *Phys. Rev. A* 82(3), 032318 (2010)
91. B. C. Ren, H. R. Wei, M. Hua, T. Li, and F. G. Deng, Complete hyperentangled-Bell-state analysis for photon systems assisted by quantum-dot spins in optical microcavities, *Opt. Express* 20(22), 24664 (2012)
92. T. J. Wang, Y. Lu, and G. L. Long, Generation and complete analysis of the hyperentangled Bell state for photons assisted by quantum-dot spins in optical microcavities, *Phys. Rev. A* 86(4), 042337 (2012)
93. Q. Liu and M. Zhang, Generation and complete nondestructive analysis of hyperentanglement assisted by nitrogen-vacancy centers in resonators, *Phys. Rev. A* 91(6), 062321 (2015)
94. G. Y. Wang, Q. Ai, B. C. Ren, T. Li, and F. G. Deng, Error-detected generation and complete analysis of hyperentangled Bell states for photons assisted by quantum-dot spins in double-sided optical microcavities, *Opt. Express* 24(25), 28444 (2016)
95. X. H. Li and S. Ghose, Hyperentangled Bell-state analysis and hyperdense coding assisted by auxiliary entanglement, *Phys. Rev. A* 96, 020303(R) (2017)

96. H. J. Briegel and R. Raussendorf, Persistent entanglement in arrays of interacting particles, *Phys. Rev. Lett.* 86(5), 910 (2001)
97. R. Raussendorf and H. J. Briegel, A one-way quantum computer, *Phys. Rev. Lett.* 86(22), 5188 (2001)
98. H. F. Wang, C. P. Yang, and F. Nori, Robust and scalable optical one-way quantum computation, *Phys. Rev. A* 81(5), 052332 (2010)
99. M. Varnava, D. E. Browne, and T. Rudolph, Loss tolerance in one-way quantum computation via counterfactual error correction, *Phys. Rev. Lett.* 97(12), 120501 (2006)
100. G. Vallone, E. Pomarico, F. De Martini, and P. Mataloni, One-way quantum computation with two-photon multiqubit cluster states, *Phys. Rev. A* 78(4), 042335 (2008)
101. M. Borhani and D. Loss, Cluster states from Heisenberg interactions, *Phys. Rev. A* 71(3), 034308 (2005)
102. Y. Tokunaga, S. Kuwashiro, T. Yamamoto, M. Koashi, and N. Imoto, Generation of high-fidelity four-photon cluster state and quantum-domain demonstration of one-way quantum computing, *Phys. Rev. Lett.* 100(21), 210501 (2008)
103. M. Yukawa, R. Ukai, P. van Loock, and A. Furusawa, Experimental generation of four-mode continuous-variable cluster states, *Phys. Rev. A* 78(1), 012301 (2008)
104. T. Yu, A. D. Zhu, S. Zhang, K. H. Yeon, and S. C. Yu, Deterministic controlled-phase gate and preparation of cluster states via singly charged quantum dots in cavity quantum electrodynamics, *Phys. Scr.* 84(2), 025001 (2011)
105. C. Zhang, Y. F. Huang, B. H. Liu, C. F. Li, and G. C. Guo, Experimental generation of a high-fidelity four-photon linear cluster state, *Phys. Rev. A* 93(6), 062329 (2016)
106. D. Loss and D. P. DiVincenzo, Quantum computation with quantum dots, *Phys. Rev. A* 57(1), 120 (1998)
107. C. Piermarocchi, P. Chen, L. J. Sham, and D. G. Steel, Optical RKKY interaction between charged semiconductor quantum dots, *Phys. Rev. Lett.* 89(16), 167402 (2002)
108. T. Calarco, A. Datta, P. Fedichev, E. Pazy, and P. Zoller, Spin-based all-optical quantum computation with quantum dots: Understanding and suppressing decoherence, *Phys. Rev. A* 68(1), 012310 (2003)
109. S. M. Clark, K. C. Fu, T. D. Ladd, and Y. Yamamoto, Quantum computers based on electron spins controlled by ultrafast off-resonant single optical pulses, *Phys. Rev. Lett.* 99(4), 040501 (2007)
110. W. Yao, R. B. Liu, and L. J. Sham, Theory of control of the spin-photon interface for quantum networks, *Phys. Rev. Lett.* 95(3), 030504 (2005)
111. A. Imamogłu, D. D. Awschalom, G. Burkard, D. P. DiVincenzo, D. Loss, M. Sherwin, and A. Small, Quantum information processing using quantum dot spins and cavity QED, *Phys. Rev. Lett.* 83(20), 4204 (1999)
112. J. R. Petta, A. C. Johnson, J. M. Taylor, E. A. Laird, A. Yacoby, M. D. Lukin, C. M. Marcus, M. P. Hanson, and A. C. Gossard, Coherent manipulation of coupled electron spins in semiconductor quantum dots, *Science* 309(5744), 2180 (2005)
113. A. Greilich, D. R. Yakovlev, A. Shabaev, A. L. Efros, I. A. Yugova, R. Oulton, V. Stavarache, D. Reuter, A. Wieck, and M. Bayer, Mode locking of electron spin coherences in singly charged quantum dots, *Science* 313(5785), 341 (2006)
114. K. D. Greve, D. Press, P. L. McMahon, and Y. Yamamoto, Ultrafast optical control of individual quantum dot spin qubits, *Rep. Prog. Phys.* 76(9), 092501 (2013)
115. J. Berezovsky, M. H. Mikkelsen, N. G. Stoltz, L. A. Coldren, and D. D. Awschalom, Picosecond coherent optical manipulation of a single electron spin in a quantum dot, *Science* 320(5874), 349 (2008)
116. K. De Greve, P. L. McMahon, D. Press, T. D. Ladd, D. Bisping, C. Schneider, M. Kamp, L. Worschech, S. Höfling, A. Forchel, and Y. Yamamoto, Ultrafast coherent control and suppressed nuclear feedback of a single quantum dot hole qubit, *Nat. Phys.* 7(11), 872 (2011)
117. M. Atature, J. Dreiser, A. Badolato, A. Högele, K. Karrai, and A. Imamoglu, Quantum-dot spin-state preparation with near-unity fidelity, *Science* 312(5773), 551 (2006)
118. J. Berezovsky, M. H. Mikkelsen, N. G. Stoltz, L. A. Coldren, and D. D. Awschalom, Picosecond coherent optical manip-ulation of a single electron spin in a quantum dot, *Science* 320(5874), 349 (2008)
119. D. Press, T. D. Ladd, B. Y. Zhang, and Y. Yamamoto, Complete quantum control of a single quantum dot spin using ultrafast optical pulses, *Nature* 456(7219), 218 (2008)
120. C. Y. Hu, A. Young, J. L. ÓBrien, W. J. Munro, and J. G. Rarity, Giant optical Faraday rotation induced by a single-electron spin in a quantum dot: Applications to entangling remote spins via a single photon, *Phys. Rev. B* 78(8), 085307 (2008)
121. C. Y. Hu, W. J. Munro, and J. G. Rarity, Deterministic photon entangler using a charged quantum dot inside a micro-cavity, *Phys. Rev. B* 78(12), 125318 (2008)
122. P. Lodahl, S. Mahmoodian, and S. Stobbe, Interfacing single photons and single quantum dots with photonic nanos-tructures, *Rev. Mod. Phys.* 87(2), 347 (2015)
123. M. J. Kastoryano, F. Reiter, and A. S. Sørensen, Dissipative preparation of entanglement in optical cavities, *Phys. Rev. Lett.* 106(9), 090502 (2011)
124. Y. Li, L. Aolita, D. E. Chang, and L. C. Kwek, Robust-fidelity atom-photon entangling gates in the weak-coupling regime, *Phys. Rev. Lett.* 109(16), 160504 (2012)
125. R. J. Warburton, Single spins in self-assembled quantum dots, *Nat. Mater.* 12(6), 483 (2013)
126. R. J. Warburton, C. S. Dürr, K. Karrai, J. P. Kotthaus, G. Medeiros-Ribeiro, and P. M. Petroff, Charged excitons in self-assembled semiconductor quantum dots, *Phys. Rev. Lett.* 79(26), 5282 (1997)
127. D. F. Walls and G. J. Milburn, Quantum Optics, Springer-Verlag, 1994

128. A. B. Young, R. Oulton, C. Y. Hu, A. C. T. Thijssen, C. Schneider, S. Reitzenstein, M. Kamp, S. Höfling, L. Worschech, A. Forchel, and J. G. Rarity, Quantum-dot-induced phase shift in a pillar microcavity, *Phys. Rev. A* 84(1), 011803 (2011)

129. H. R. Wei and F. G. Deng, Universal quantum gates on electron-spin qubits with quantum dots inside single-side optical microcavities, *Opt. Express* 22(1), 593 (2014)

130. X. B. Zou and W. Mathis, Generating a four-photon polarization-entangled cluster state, *Phys. Rev. A* 71(3), 032308 (2005)

131. Q. A. Turchette, C. J. Hood, W. Lange, H. Mabuchi, and H. J. Kimble, Measurement of conditional phase shifts for quantum logic, *Phys. Rev. Lett.* 75(25), 4710 (1995)

132. J. P. Reithmaier, G. Sek, A. Löffler, C. Hofmann, S. Kuhn, S. Reitzenstein, L. V. Keldysh, V. D. Kulakovskii, T. L. Reinecke, and A. Forchel, Strong coupling in a single quantum dot-semiconductor microcavity system, *Nature* 432(7014), 197 (2004)

133. S. Reitzenstein, C. Hofmann, A. Gorbunov, M. Strauss, S. H. Kwon, C. Schneider, A. Loffler, S. Hofling, M. Kamp, and A. Forchel, AlAs/GaAs micropillar cavities with quality factors exceeding 150.000, *Appl. Phys. Lett.* 90(25), 251109 (2007)

134. J. R. Petta, A. C. Johnson, J. M. Taylor, E. A. Laird, A. Yacoby, M. D. Lukin, C. M. Marcus, M. P. Hanson, and A. C. Gossard, Coherent manipulation of coupled electron spins in semiconductor quantum dots, *Science* 309(5744), 2180 (2005)

135. A. B. Young, C. Y. Hu, and J. G. Rarity, Generating entanglement with low-Q-factor microcavities, *Phys. Rev. A* 87(1), 012332 (2013)

136. N. K. Langford, T. J. Weinhold, R. Prevedel, K. J. Resch, A. Gilchrist, J. L. O'Brien, G. J. Pryde, and A. G. White, Demonstration of a simple entangling optical gate and its use in Bell-state analysis, *Phys. Rev. Lett.* 95(21), 210504 (2005)